Multicarrier waveforms classification with deep neural networks

Zhe Deng, Jing Lei✉, Zehan Wan, and Yuliang Dong
Department of Communication Engineering, College of Electronic Science and Engineering, National University of Defense Technology, Changsha, China
✉Email: leijing@nudt.edu.cn

Automatic modulation classification (AMC) plays an important role in various applications such as cognitive radio and dynamic spectrum access. Many research works have been exploring deep learning (DL) based AMC, but they primarily focus on single-carrier signals. With the advent of various multicarrier waveforms, the authors propose to revisit DL-based AMC to consider the diversity and complexity of these novel transmission waveforms in this letter. Specifically, the authors develop a novel representation of multicarrier signals and use suitable networks for classification. In addition, to cope with non-target signals, support vector data description (SVDD) is applied with the activations of the networks' hidden layer. Experimental results demonstrate the effectiveness of the proposed scheme.

Introduction: With orthogonal frequency division multiplexing (OFDM) being used, multicarrier waveforms can achieve high data rate and spectral efficiency in wireless mobile networks. As enhanced versions of OFDM, several waveforms have been proposed by filtering and precoding. In addition to OFDM and single carrier (SC), we focus on two types of waveforms:

- Filtering-based multicarriers: filter bank multicarrier (FBMC)[1], universal filtered multicarrier (UFMC)[2], and filtered orthogonal frequency division multiplexing (F-OFDM)[3].
- Precoding-based multicarriers: orthogonal time frequency space (OTFS)[4], hybrid carrier (HC)[5], OTFS extended by weighted-type fractional Fourier transform (WFRFT-OTFS)[6].

Deep learning (DL) architectures have recently played an important role in modulation classification. In [7, 8], simple and proper convolutional neural network (CNN), long short-term deep neural network (CLDNN), and visual geometry group network (VGGNet) are adopted to distinguish different modulation types. The results show that the DL-based methods have superiority over the conventional feature-based methods. In [9], the modulated signals are converted into cyclic spectra and constellation diagrams, and classified by neural networks. In [10], a new network architecture that combines a frequency selection module and a convolutional neural network (CNN) is proposed to handle raw signal data with carriers. In [11], constellation diagrams of signals are used for the classification and achieve significant performance. These AMC methods based on DL mainly focus on single-carrier waveforms. However, few works were reported on the use of DL models for OFDM variants classification. In addition, a complete identification scheme should have the ability to detect anomalies, because the number of signal categories received in practice is much larger than the candidate set size.

Signal constellation diagrams lose the time domain information of the signal, but still, provide enough information gain for modulation identification. Hence if we keep the time domain information, it should theoretically achieve better results. Inspired by this, we propose to encode complex signals as constellation clouds and then transform them into data formats with a gridlike topology, i.e. 3-D pictures, which facilitate the use of prevalent DL network models for classification. The responses of networks' hidden layer are taken as signals' features, and then support vector data description (SVDD)[12] is used for anomaly detection.

Data conversion and appropriate networks: General neural networks accept only real-valued inputs, so an N points complex signal is often divided into in-phase and quadrature (I/Q) parts, thus turning into an $N \times 2$ vector. Mapping the samples to a complex plane, we can obtain the constellation diagram, which is an effective representation and has been successfully applied to AMC in [11]. However, these points have an order, and the modulated signal, which already has two dimensions, in-phase and quadrature, will become a three-dimensional vector when the time dimension is added. Specifically, by concatenating a position vector (e.g., $1/N \times [1\ 2\ \ldots\ N]^{\mathrm{T}}$) into an original vector, we get an $N \times 3$ vector. No matter how we swap the order, this new vector represents the same 3-D object, that is, the constellation cloud of this signal. Figure 1 (b) give an example of a constellation cloud, which is generated from 4096 points of UFMC signal (see Figure 1(a)) with the SNR at 30 dB.

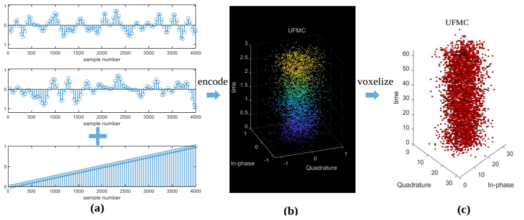

Fig 1 *Complex samples and constellation clouds for UFMC signal at SNR=30dB. (a) Complex signal samples and position vector. (b) Constellation cloud. (c) Voxelization result.*

A common method for classifying 3-D objects is voxelization, which means that the 3-D space is gridded and the number of points falling into the grids is taken as the values of the grids, as shown in Figure 1(c). So a 3-D image can be obtained, and then use a simple 3-D convolutional neural network architecture to perform classification. Figure 2(a) illustrates the structure of VoxNet[13].

However, there is a trade-off in the voxelization approach. The more refined the voxelization, the higher accuracy, but the higher complexity. Voxelization is always accompanied by information loss, so PointNet[14] emerges as a groundbreaking approach. With several multilayer perceptrons, PointNet can generate stable features from point cloud data directly and then classify point clouds by fully connected layers. In experiments, we use an upgraded version of PointNet, PointNet++[15], which performs sampling and grouping to divide the original point cloud data into local region sets, and then use the mini-PointNet to extract the features of the data. We attached the classification module at the back end of PointNet++ to obtain a proper structure, as shown in Figure 2(b).

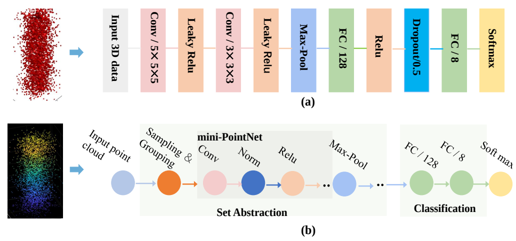

Fig 2 *DL networks for constellation clouds. (a) VoxNet. (b) PointNet++.*

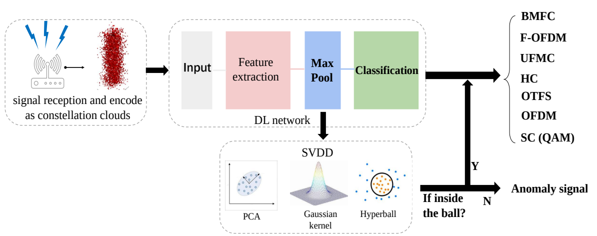

Fig 3 *Multicarrier waveforms classification scheme.*

Anomaly detection method: The networks can identify the input signal as one of the candidate set, but we need to judge if the signal belongs to the candidate set first. After inputting target signals into the network, the activations of a hidden layer (e.g., the last max pooling layer) are seen as extracted features. The features' dimension is reduced by principal component analysis (PCA) and then a hypersphere is constructed

Table 1. Filter properties of filtered multicarrier waveforms.

	Filter type	Filter length	Number of subbands	Subbands size	Overlapping factor
UFMC	Dolph-Chebyshev	23	4	8	1
F-OFDM	Truncated Sinc	33	15	4	1
FBMC	Phydyas	7	48	1	4

using SVDD. When identifying a new signal, we just calculate the distance between the signal's feature and the hypersphere core to determine whether the signal belongs to the target set. The features generally do not follow a spherical distribution, so a Gaussian kernel function is used, and the kernel parameters and loss coefficients are optimized by genetic algorithm. In summary, our proposed multicarrier waveforms classification scheme is shown in Figure 3.

Experiment setup: We generated a multicarrier waveforms data set of 8 types. The subcarriers' modulation type includes 4QAM, 16QAM, 64QAM, and 256QAM. Subcarrier spacing is 20 kHz, and the oversampling rate is from one to eight. The number of resources for OTFS and IDFT size for OFDM are both 64. Parameters in Table 1 are adopted for filtering-based multicarriers. The cyclic prefix length is 4. The SNR is from 0 to 30 dB for a total of 16 integer types. 1000 samples are generated in each parameter and channel condition, with 4096 points per sample. The modulation set is denoted as:

$$\Omega = \{\mathrm{FBMC, UFMC, F-OFDM, OTFS, HC, WFRFT-OTFS, SC}\}$$

Phase shift keying (PSK) modulation signals are used as anomaly signals. The anomaly set is denoted as:

$$\bar{\Omega} = \{\mathrm{BPSK, QPSK, 8PSK, O-QPSK}, \pi/4-\mathrm{QPSK}\}$$

Among the dataset, 80% of them are used for training, 10% of them are used for validation, and the rest are used as the test set. Alternatively, the $N \times 2$ vector can be treated as a single-channel picture. Hence, to verify the effectiveness of our method, we compare the proposed method with modified ResNet[16] and DenseNet[17], which are commonly used in image processing. The baseline networks both use only first 18 convolutional layers, denoted as ResNet18 and DenseNet18.

Performance evaluation: Since the resolution of voxelization should be neither too small nor too large, we discuss its impact on classification accuracy. Different sizes of 3-D pictures, including $32 \times 32 \times 64$, $16 \times 16 \times 128$, and $16 \times 16 \times 256$, are considered. We plot the average accuracy of networks with SNRs to explore the adaptability to various SNRs (see Figure 4(a)). We can see that SNR level has a significant impact on accuracy. When the SNR is higher than 10 dB, all networks perform close to each other, with almost no classification error, and VoxNet outperforms other networks. At low SNRs, ResNet18 and DenseNet18 exhibit greater resilience, while VoxNets suffer a dramatic drop in performance. However, when SNR is less than 10 dB, even if the modulation type could be identified correctly, high-order QAM signals' BER would be higher than 10^{-2}, making it difficult to recover the information and the identification would be meaningless. PointNet++ performs slightly worse than VoxNets at higher SNRs, but has stronger noise tolerance. VoxNet with input size $16 \times 16 \times 128$ uses a smaller input size than the other two VoxNets, but achieves fairly good result and is an ideal choice. To further investigate the classification accuracy of this network in different modulation formats, the confusion matrix is shown in Figure 4(b). The row label of the matrix indicates the target class, and the columns indicate the output class. We can see that the proposed network can achieve a good result on filtering-based multicarriers, but poorer on precoding-based multicarriers, probably because precoding-based signals are inherently closer to each other. In addition, we draw anomaly detection accuracy of networks on the whole test set and the proportion of various error types, as shown in Figure 5. It can be seen that the voxnet-based SVDD scheme has the optimal detection performance, with errors mainly concentrated in the 8PSK and SC-FDE (QAM) types. In terms of the modulation mechanism, high-order PSK signals are inherently close to low-order QAM signals.

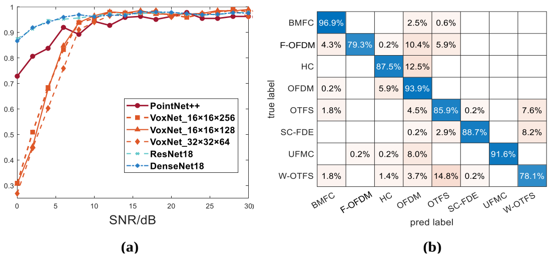

Fig 4 *Recognition performance of networks. (a) Classification accuracies in differernt SNRs. (b) Confusion matrix for VoxNet_$16 \times 16 \times 128$.*

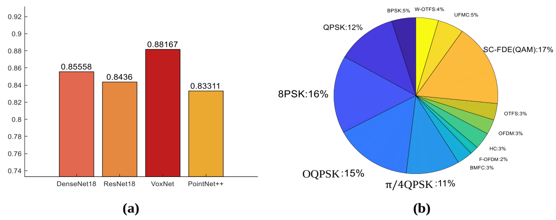

Fig 5 *Anomaly detection performance of networks. (a) Average detection accuracy on the whole test set. (b) Proportion of different error types.*

Computational complexity analysis: The major worry about using the DL in communications systems might be huge computational complexity. Fortunately, only the testing phase is frequently applied when implementing the DL in communications systems. The training phase is usually conducted beforehand and does not incur much computational burden. The computational complexity of the four models is evaluated by calculating the test time consumption and the number of learned parameters. As shown in Figure 6, we calculated test time per sample and learnable parameters of the four models: PiontNet++ 0.05s and 0.6M, VoxNet 0.00015s and 2M, ResNet18 0.0032s and 5M, DenseNet18 0.0014s and 3M. VoxNet is deployable in most scenarios with the fastest prediction speed and relatively few parameters, while PiontNet++ requires a reduction in time complexity before practical application.

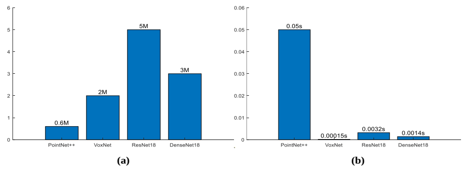

Fig 6 *Computational complexity comparision of networks. (a) The number of learned parameters. (b) Test time consumption per sample.*

Conclusion: In this letter, we propose a data conversion method to generate constellation clouds from complex signals, and then use proper networks to identify them for multicarrier waveforms classification. SVDD with a Gaussian kernel is used to prevent misclassification of anomalous signals by a hyperspherical description of the target dataset. The results show that our classification method achieves the equivalent accuracy but with less complexity than conventional dl networks. SVDD can identify non-target signals precisely and prevent them from moving on to the classification step. In future work, the impact of time-frequency dual selection channel interference will be investigated.

Acknowledgments: This work was supported by the National Natural Science Foundation of China. 6217072012.

Received: DD MMMM YYYY *Accepted:* DD MMMM YYYY doi: 10.1049/ell.10001

References

1. Bellanger, M.: Fs-fbmc: An alternative scheme for filter bank based multicarrier transmission. In: 2012 5Th international symposium on communications, control and signal processing, pp. 1–4. IEEE (2012)
2. Zhang, L., et al.: Subband filtered multi-carrier systems for multi-service wireless communications. IEEE Transactions on Wireless Communications 16(3), 1893–1907 (2017)
3. Abdoli, J., Jia, M., Ma, J.: Filtered ofdm: A new waveform for future wireless systems. In: 2015 IEEE 16th International Workshop on Signal Processing Advances in Wireless Communications (SPAWC), pp. 66–70. IEEE (2015)
4. Raviteja, P., et al.: Practical pulse-shaping waveforms for reduced-cyclic-prefix otfs. IEEE Transactions on Vehicular Technology 68(1), 957–961 (2018)
5. Wang, Z., et al.: Ber analysis of stbc hybrid carrier system based on wfrft with frequency domain equalization. Science China Information Sciences 61(8), 1–13 (2018)
6. Wang, Z., Chen, X., Ning, X.: Ber analysis of integrated wfrft-otfs waveform framework over static multipath channels. IEEE Communications Letters 25(3), 754–758 (2020)
7. O'Shea, T.J., Roy, T., Clancy, T.C.: Over-the-air deep learning based radio signal classification. IEEE Journal of Selected Topics in Signal Processing 12(1), 168–179 (2018)
8. Liu, X., Yang, D., El Gamal, A.: Deep neural network architectures for modulation classification. In: 2017 51st Asilomar Conference on Signals, Systems, and Computers, pp. 915–919. IEEE (2017)
9. Wu, H., et al.: Convolutional neural network and multi-feature fusion for automatic modulation classification. Electronics Letters 55(16), 895–897 (2019)
10. Liu, W., et al.: Automatic modulation classification with deep learning-based frequency selection filters. Electronics Letters 56(21), 1144–1145 (2020)
11. Peng, S., et al.: Modulation classification based on signal constellation diagrams and deep learning. IEEE transactions on neural networks and learning systems 30(3), 718–727 (2018)
12. Tax, D.M., Duin, R.P.: Support vector data description. Machine learning 54(1), 45–66 (2004)
13. Maturana, D., Scherer, S.: Voxnet: A 3d convolutional neural network for real-time object recognition. In: 2015 IEEE/RSJ international conference on intelligent robots and systems (IROS), pp. 922–928. IEEE (2015)
14. Qi, C.R., et al.: Pointnet: Deep learning on point sets for 3d classification and segmentation. In: Proceedings of the IEEE conference on computer vision and pattern recognition, pp. 652–660. (2017)
15. Qi, C.R., et al.: Pointnet++: Deep hierarchical feature learning on point sets in a metric space. Advances in neural information processing systems 30 (2017)
16. He, K., et al.: Deep residual learning for image recognition. In: Proceedings of the IEEE conference on computer vision and pattern recognition, pp. 770–778. (2016)
17. Huang, G., et al.: Densely connected convolutional networks, vol. 2017-January, pp. 2261 – 2269. (2017)